A Combined Infrared Photodissociation and Theoretical Study of the Interaction of Ethanol with Small Gold Clusters

Geoffrey M. Koretsky and Mark B. Knickelbein*

Chemistry Division, Argonne National Laboratory, Argonne, Illinois 60439

Roger Rousseau* and Dominik Marx

Lehrstuhl für Theoretische Chemie, Ruhr−Universität Bochum, 44780 Bochum, Germany

Received: August 1, 2001; In Final Form: October 8, 2001

The infrared photodissociation spectra of $Au_n(C_2H_5OH)_m$ (n = 3, 9, 11; m = 1−4) complexes have been recorded in the 9−11 μm region. The ethanol vibrational band frequencies are observed to be invariant with the size of the underlying gold clusters, indicating that local, rather than global, interactions determine the frequency shifts from the gas-phase values. Experimental results are compared with electronic structure calculations for both $Au_3(C_2H_5OH)$ and $Au_3(CH_3OH)$. From these calculations a model for the binding of the single alcohol to the gold cluster is proposed which qualitatively accounts for many of the experimental observations.

1. Introduction

The study of metal clusters and their interactions with atoms and small molecules allows detailed, tractable investigations of the elementary processes and intermediates that occur during chemisorption reactions, for example those of relevance to catalysis.[1,2] Survey studies have shown that the reactivity trends of the coinage metal clusters, Cu_n, Ag_n, and Au_n, generally mirror those of the corresponding bulk metals, with nondissociative chemisorption (i.e., simple association reactions) being the most commonly observed type of chemical behavior at room temperature and below.[2−9] However, unlike bulk coinage metal surfaces, small coinage metal clusters possess unique structural and electronic characteristics that might be expected to influence reactivity rates and pathways for certain classes of reactions. The manifestation of electronic shell filling in the *physical* properties of coinage metal clusters is well documented. For example, measurements of ionization potentials and electron affinities, as well as observations of relative stabilities toward unimolecular dissociation, have revealed sudden discontinuities of these properties at special cluster sizes.[10−15] These anomalies are attributable to the delocalization of the metals' valence electrons throughout the volume of the clusters and the resulting organization of electron levels into shells and subshells.[16−19] In selected cases, it has been observed that this electronic shell filling phenomenon is reflected in chemical behavior as well, for example in stability/abundance studies of Cu_nCO^+,[6] Cu_nCO^-,[20] and $Au_n(CO)_m^-$,[21] and in reactivity studies of Cu_n and Au_n with O_2,[5,22,23] where shell closing-related anomalies have been observed. However electronic shell structure is not the only factor determining chemical behavior; coinage metal clusters also display nonbulklike *geometric* structures that vary substantially from one size to the next.[24−30] The current understanding of the roles of electronic vs geometric structure in determining the chemical behavior of coinage metal clusters toward small molecules is incomplete. In the present study we investigate these effects on small gold clusters using ethanol as a probe molecule.

Infrared (IR) spectroscopy of surface-adsorbed molecules is a sensitive tool for probing the nature of the substrate−adsorbate interaction. This technique, originally developed for investigating chemisorption on macroscopic surfaces, has recently been extended to *molecular surfaces*, as provided by small metal clusters. Infrared photodissociation studies have been reported for $Au_n(CH_3OH)_m^+$ (n = 1−10,15 m = 1−3)[31−33] and for $M_n(CD_3OH)_m$ and $M_n(CD_3OD)_m$, M = Cu, Ag, and Au.[9] The IR spectra indicate that methanol binds molecularly to the underlying coinage metal clusters. For both Au_n^+ and Au_n species, the C−O stretching vibration of adsorbed methanol was observed to shift to higher frequencies with increasing coverage, suggesting that the adsorbed methanol molecules interact with one another in these complexes. In contrast to the interaction between CO molecules and positively charged copper clusters,[6] for methanol chemisorbed onto Au_n^+ clusters it was found that electronic shell effects were not the underlying cause for the observed trends in shifts in the C−O stretching frequencies.[32−34] Rather the strength of the Au_n−methanol interaction, theoretically ascribed to a direct Au−O coordination bond, was sensitive to the *geometrical* structure of the gold cluster, with planar clusters providing larger frequency shifts then three-dimensional species due to the larger coordination number of the Au atom which was engaged in the binding for the latter case. This effect was not observed in neutral methanol cluster adducts owing to the weaker nature of the cluster molecule interaction.[9,34] The current work is intended to further test the previously proposed binding model with respect to shifts in ionization potential and the bonding of a larger alcohol species—ethanol. In this work, the trends in both C−O stretching frequency and ionization potential shift are examined both theoretically, via electronic structure calculations, and experimentally via infrared photodissociation spectra and photoionization mass spectra of complexes formed from the reaction of selected gold clusters with ethanol: $Au_n(C_2H_5OH)_m$.

* Corresponding author.

10.1021/jp0129636 CCC: $20.00
Published on Web 11/20/2001

2. Experimental Methods

The experimental apparatus and methods used to record infrared photodissociation spectra have been described in detail previously.[35] Briefly, gold clusters were generated by pulsed laser vaporization (Nd:YAG second harmonic, 25 mJ/pulse) from a foil target within a continuous-flow cluster source. The flow tube where cluster growth and thermalization occur (helium, 10 Torr) was maintained at 65 ± 5 K by a helium refrigerator. Ethanol complexes of the coinage metal clusters were formed by adding a trace of C_2H_5OH in helium to the cluster source. The resulting partial pressure of ethanol in the flow tube was approximately 10 mTorr under typical flow conditions.

Following expansion through a 0.10 cm diameter nozzle, a molecular beam containing the clusters was formed, which ultimately entered into a detection chamber held at $<10^{-6}$ Torr. Here the beam was crossed at 90° by a collimated ArF (probe) laser ($h\nu = 6.4$ eV) that ionized the clusters for time-of-flight (TOF) mass analysis. Prior to every other ArF laser pulse, a line-tunable, carbon dioxide (pump) laser counterpropagated the molecular beam with an effective interaction time of approximately 200 μs. The relative depletion of the cluster complexes was measured by pulsing the pump laser at one-half the probe laser repetition rate and concurrently recording two TOF spectra, a *reference* TOF spectrum obtained with the ArF probe laser only, and a *depletion* TOF spectrum obtained using both pump+probe lasers. The relative pump laser fluence F was measured by reflecting a portion of the CO_2 laser output into a pyroelectric energy detector. Effective cross sections σ were calculated at each wavelength from the measured depletion, D, assuming a first-order saturation behavior: $D = [1 - e^{-\sigma F}]$. The validity of this approach for infrared multiphoton dissociation experiments such as those described here is discussed in ref 35.

3. Computational Approach

To further investigate both ionization potential energy shifts as well as trends in the C−O stretching frequency upon adsorption of small chain aliphatic alcohols to Au_n clusters we have also performed theoretical electronic structure calculations using Au_3 as a model cluster substrate. Based upon our previous results[34] it is sufficient to examine only static configurations due to the fact that each cluster−alcohol adduct whence formed does not isomerize on the picosecond time scale. The contribution of anharmonicity in the C−O stretching frequency for neutral Au_n-alcohol adducts and the isolated alcohol is almost identical and therefore, unlike the positively charged analogues,[32,34] only harmonic frequencies need to be considered. In addition, the shift in C−O frequencies for neutral species were found to be insensitive to cluster size. Thus it will be sufficient to only examine the static isomers of a single cluster−alcohol adduct.

We have thus performed static geometry optimization and harmonic vibrational analysis for various isomers of Au_3, methanol, and ethanol as well as the adducts formed between these species employing the Gaussian 98 quantum chemistry package.[36] Gold is represented by a "small core" energy-consistent semi-relativistic pseudo-potential[37] of the Stuttgart group with 19 electrons in the valence shell and the associated basis set. The remaining atoms are provided with a 6-311G basis set supplemented by (2d,2p) polarization.[38−40] Calculations are performed within the framework of Density Functional Theory (DFT)[41,42] where the gradient corrections of Becke for exchange[43] and Perdew for correlation[44] (BP86) have been employed which are identical to those used in our previous work.[32,34] To roughly estimate the degree to which dispersion forces affect the bonding and physical properties of the adducts, calculations employing the post Hartree−Fock MP2 method[45] are also presented. For an application and comparison of these prescriptions to the interaction of Au_n clusters and short chain thiol and thiolate molecules and comparison to pseudo-potential methods see ref 46. Spin−orbit coupling effects have been neglected in all calculations. The deviation of the electronic state from a pure doublet was minimal as measured by values of the spin operator where the maximum deviation from $S^2 = 0.75$ (pure doublet) was found to be at most 0.02 indicating negligible spin contamination. The starting configuration of each cluster−alcohol adduct is obtained by placing the alcohol molecule in a configuration analogous to that found in our previous work[32,34] and relaxing the geometry to the nearest local minimum on the potential energy surface. For each isomer of Au_3 the alcohol was attached to each symmetry-independent Au atom of that isomer to obtain a final adduct species. Alternate conformations of the ethanol molecule, where the orientation of the terminal methyl group relative to the hydroxyl group were also investigated for the lowest energy adduct of the Au_3−ethanol species.

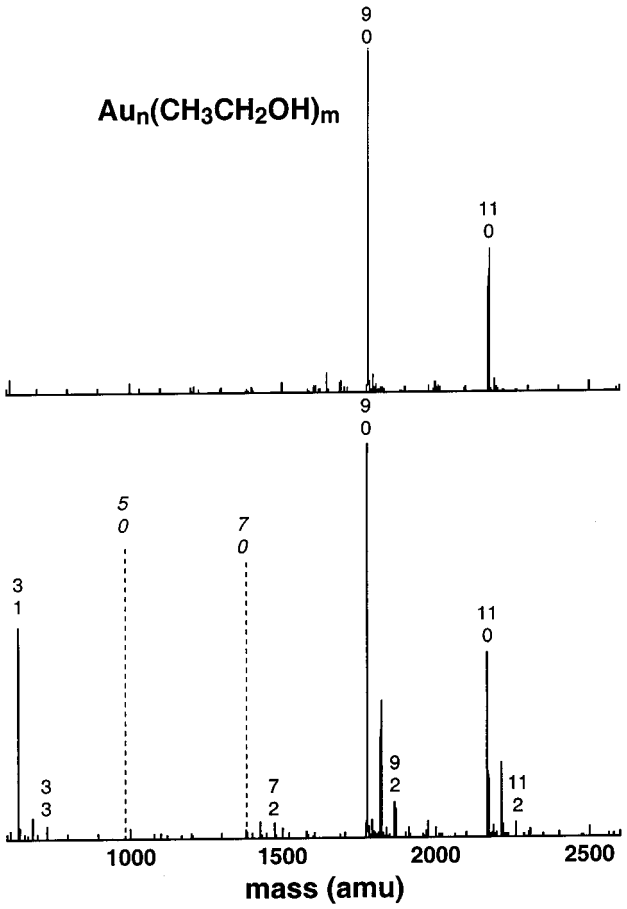

Figure 1. Photoionization time-of-flight mass spectrum of gold clusters at 193 nm (6.4 eV). Top trace: helium carrier gas only. Bottom trace: ethanol added to carrier gas. Au_n and $Au_n(C_2H_5OH)_m$ complexes are labeled according to $^{n}_{m}$. The expected locations of bare Au_5 and Au_7 are indicated. Bare Au_3 is also absent at this ionization wavelength.

4. Results and Discussion

4.1. Photoionization Mass Spectra. A photoionization time-of-flight mass spectrum of $Au_n(C_2H_5OH)_m$ recorded at 193 nm (6.4 eV) is shown in Figure 1. The presence of TOF peaks corresponding to ethanol complexes of gold clusters which

cannot be ionized at 193 nm in their bare form demonstrates that adsorption of ethanol onto the clusters effectively lowers Au_n ionization potentials (IPs). For example, while Au_3 and Au_7 are not observed in the 193 nm TOF mass spectrum due to their relatively high ionization potentials, their corresponding ethanol complexes are present, as shown in Figure 1. The absence of ethanol complexes of the even-*n* gold clusters in this size range implies that their IPs are significantly greater than 6.4 eV, while the IPs of certain odd-*n* clusters are apparently close enough to 6.4 eV that they can be ionized when complexed with ethanol. Although no accurate determinations of gold cluster IPs have been presented to date, Collings et al.[47] have observed that Au_n ($n = 7$, 9, 11, and 13) produced at room temperature can be ionized by a single 6.4 eV photon. The top trace in Figure 1 shows that with the cluster source maintained at ~65 K, only Au_9 and Au_{11} are photoionized in the present experiment. The room-temperature source employed by Collings et al. apparently produced clusters containing sufficient amounts of internal energy to reduce the ionization thresholds below 6.4 eV.[48] Simple electrostatic considerations show that a polar molecule adsorbed with its dipole moment directed toward the cluster will result in an IP decrease.[49] The observation that ethanol effectively lowers the IPs of gold clusters verifies that just as on the corresponding macroscopic coinage metal surfaces, ethanol adsorbs to these clusters dipole-down, as was observed for methanol on Cu_n, Ag_n, and Au_n.[9]

4.2. Infrared Photodissociation Spectra. Surface studies have shown that methanol adsorbs to a Au(110) surface with an adsorption enthalpy of 56 kJ/mol (0.58 eV/molecule).[50] Assuming that this value provides a reasonable estimate of gold cluster−ethanol binding energies, absorption of six or more infrared photons ($h\nu \approx 0.1$ eV at $\lambda = 10$ μm) is required to reach the dissociation threshold of the $Au_n(C_2H_5OH)_m$ complexes. It has been shown, however, that even in such multiphoton studies, the variation of photodepletion with fluence mimics that of a simple one-photon photodissociation process, and is thus well described by first-order (sigmoidal) saturation kinetics behavior[35] (cf. Section 2). The present study was conducted using sufficiently low ethanol flows to ensure that the product distribution was narrow ($m \leq 4$) and skewed toward low *m*, thus minimizing distorting effects of serial decomposition.[35]

The infrared photodissociation spectra of $Au_n(C_2H_5OH)_m$ complexes for $n = 3$, 9, and 11 are shown in Figures 2−4. For the monoadducts, there is a single strong depletion band at or slightly to the red of 1030 cm^{-1}. (The gap in the CO_2 laser tuning range prevented frequencies between 990 and 1027 cm^{-1} from being investigated.) This feature is within a few cm^{-1} of a strong absorption band observed for gas-phase ethanol[51,52] as well as for ethanol molecules adsorbed on large argon clusters[53] and trapped in argon matrixes at 20 K.[54] As shown in Figures 2−4, a progressive broadening and blue shift of this depletion band is observed as ethanol coverage increases. For larger ethanol coverages an additional, weaker band is observed in the 1080−1090 cm^{-1} region. The assignment of the ethanol vibrational features in the 1000−1100 cm^{-1} region is complicated by the fact that ethanol molecules appear as two conformers—*gauche* and *anti*—which differ in the orientation of the hydroxyl group with respect to the methyl group. The gauche conformer displays IR fundamentals around 1058 cm^{-1} [r(CH_3) + δ(OH)], 1064 cm^{-1} [ν(CCO) + δ(OH)], and 1126 cm^{-1} [r(CH_2) + r(CH_3)], whereas for the anti conformer fundamentals appear around 1089 cm^{-1} [ν(CCO) + r(CH_3)] and 1032 cm^{-1} [ν(CCO) + r(CH_3)].[52] Because the observed

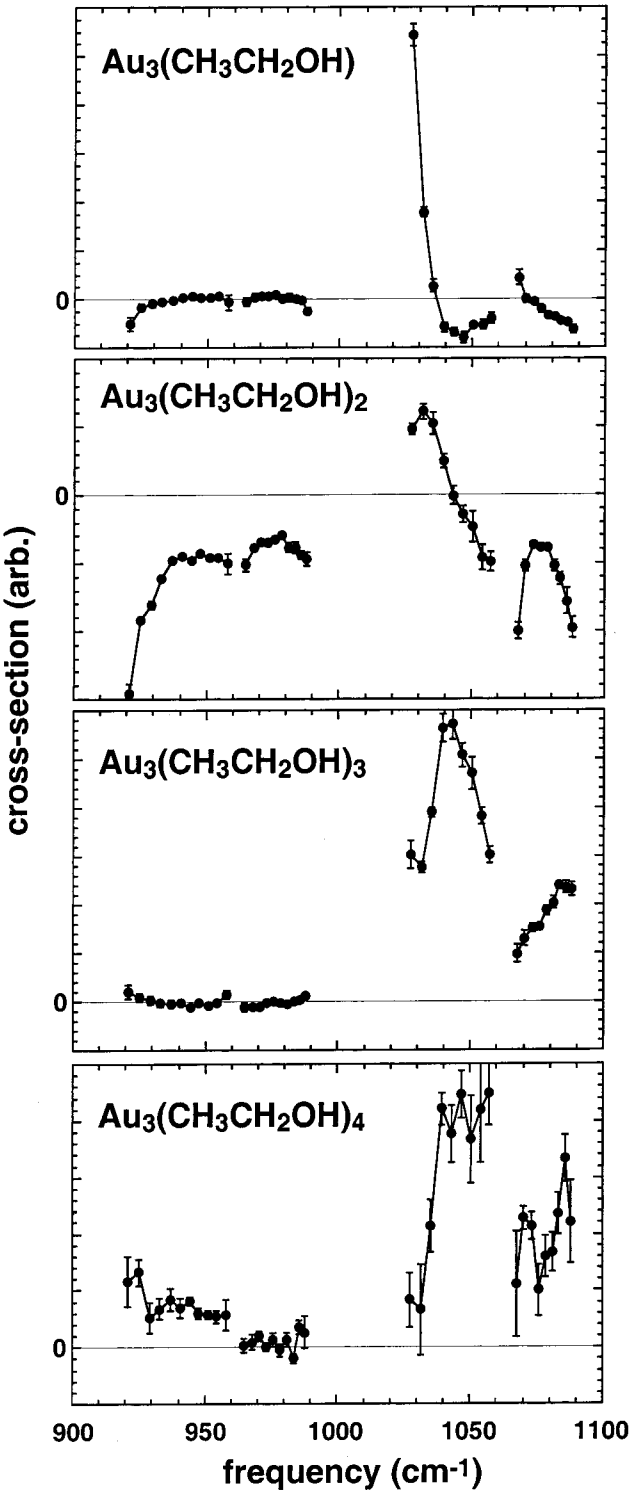

Figure 2. Infrared photodissociation spectra of $Au_3(CH_3CH_2OH)_m$ complexes.

$Au_n(CH_3CH_3OH)_m$ depletion bands frequencies correlate well with those of the anti conformer of gas-phase ethanol, it is tempting to conclude that ethanol is adsorbed as the anti conformer within the $Au_n(CH_3CH_3OH)_m$ complexes. However, it must be anticipated that the fundamentals of the adsorbed species will be shifted somewhat from those of the gas-phase molecule. For the Au_nCD_3OH and Au_nCD_3OD species, the C−O stretching frequency (corresponding to ν(CCO) in ethanol) was shifted downward ~25 cm^{-1} from the gas-phase value.[9] If a shift of the same magnitude is assumed to occur for

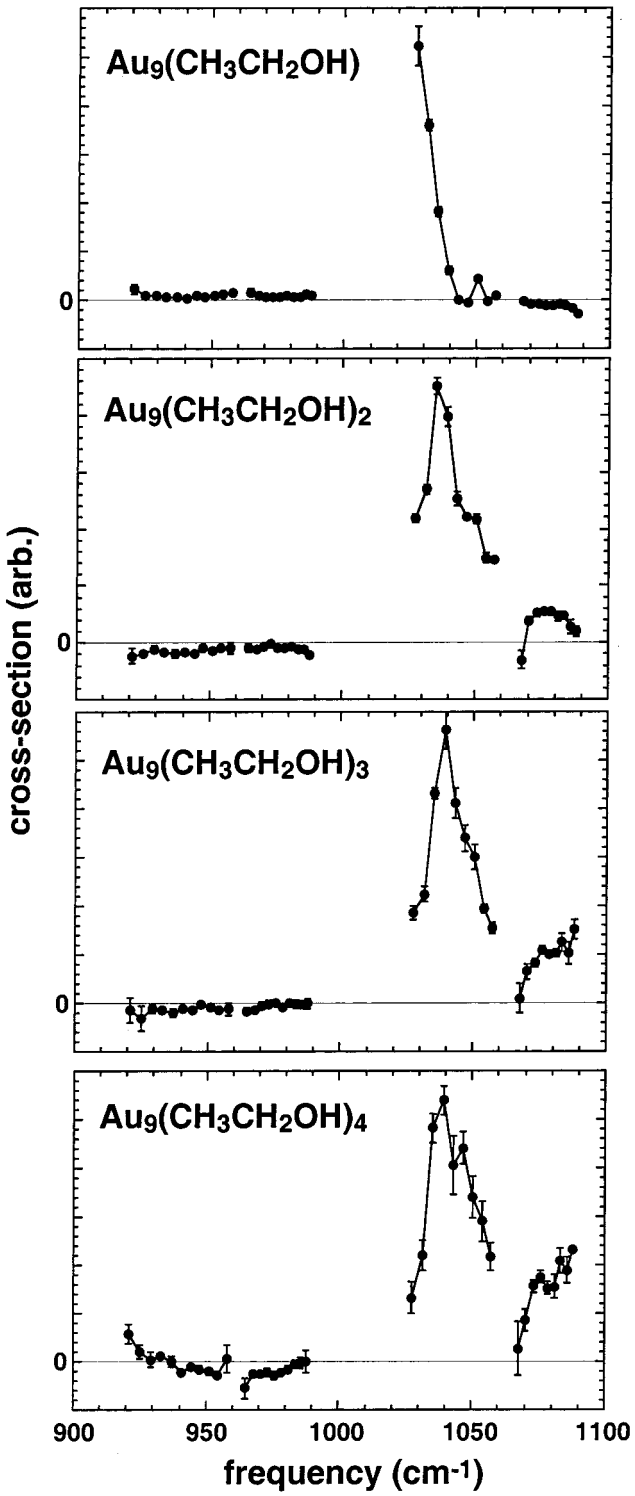

Figure 3. Infrared photodissociation spectra of $Au_9(CH_3CH_2OH)_m$ complexes.

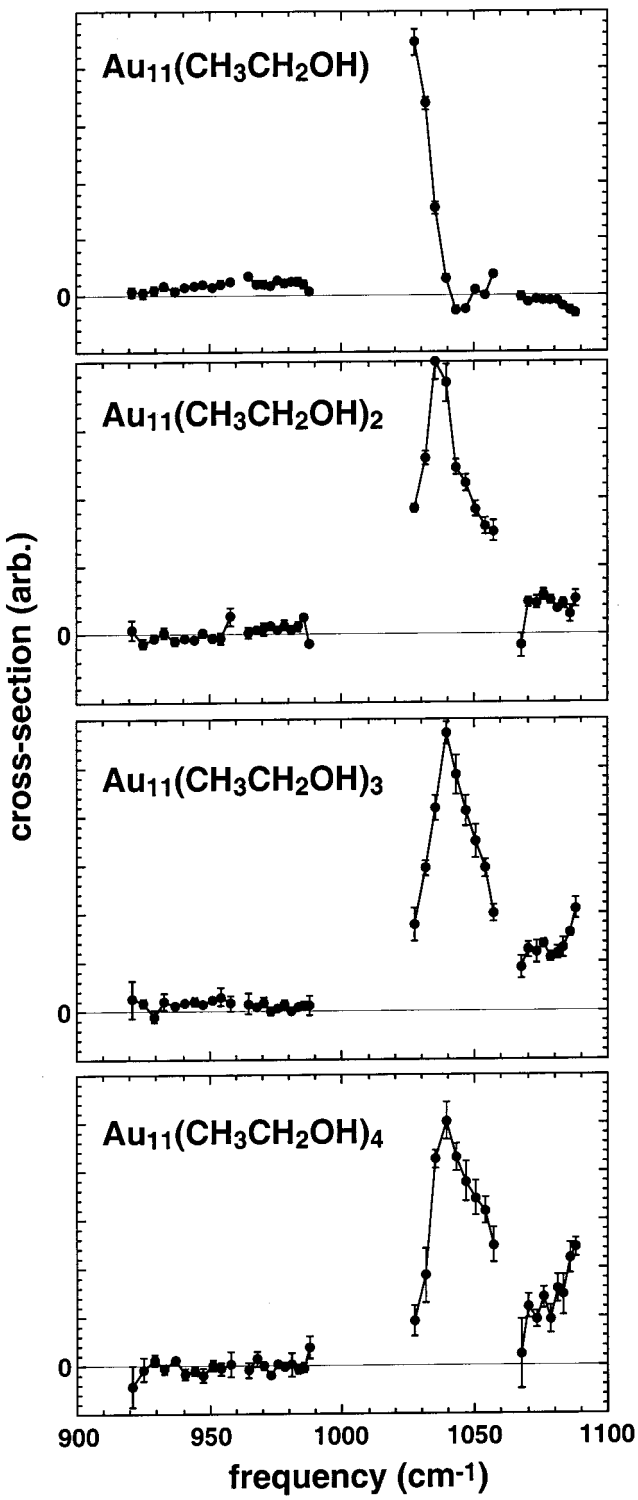

Figure 4. Infrared photodissociation spectra of $Au_{11}(CH_3CH_2OH)_m$ complexes.

$Au_nCH_3CH_3OH$ complexes, the observed band near 1030 cm^{-1} could be reasonably assigned to the ν(CCO) + δ(OH) and/or r(CH_2) + r(CH_3) modes of the gauche confomer, lying at 1064 and 1058 cm^{-1}, respectively. It is possible that the observed bands are (unresolved) combinations of both anti and gauche bands. Matrix isolation studies[52] have shown that anti↔gauche interconversion of ethanol can take place at temperatures below 30 K, although whether this result is transferable to Au_n-adsorbed ethanol is unclear. Theoretical investigation of the two ethanol conformers is presented below.

The observation of broadening and upward frequency shifts of the absorption bands with increasing m is analogous to the behavior seen in Au_n(methanol)$_m$ complexes.[9] Because the spectra of the monoadducts display only a single depletion band in the frequency range of this experiment, we can assume either that the ethanol molecules adsorb to a single type of site on the cluster surface or that the band position is independent of the type of surface site occupied. The observed broadening and blue-shifting with increasing ethanol coverage is similar to the broadening and blue-shifting of the infrared

spectra of $(C_2H_5OH)_n$ and $(C_2H_5OH)_n \cdot Ar_m$ species ($n = 2$ and 3).[53] We believe this is due to the interaction among the ethanol molecules on the surfaces of the gold clusters, forming dimers and higher oligomers, as proposed for Au_n(methanol)$_m$.[9] The binding energies of the various ethanol dimer donor−acceptor isomers have been calculated lie in the 0.29−0.34 eV range,[53] a substantial fraction of the 0.56 eV adsorption energies estimated for the Au_n−ethanol interaction.[50]

The similarity of the band shifts, $\Delta\nu$, among gold clusters of differing size implies an insensitivity of cluster−adsorbate interaction to the structure of the underlying metal cluster. While there are no direct experimental determinations of the structures of small gold clusters, electronic structure calculations and studies based on empirical many-body potentials indicate that they exhibit a variety of dissimilar structures as a function of size, rather than a common structural motif.[29,30,32,46,55−57] For example, molecular dynamics studies[30] using an empirical many-body potential predict that Au_3 is an equilateral triangle (D_{3h}), while Au_9 is predicted to be a tricapped trigonal prism (D_{3h}) and Au_{11} an octadecahedron (C_{2v}). Note that higher level DFT studies predict Au_3 is an isosceles triangle having C_{2v} symmetry (vide infra). The invariance of the observed absorption frequencies with cluster size suggests that the cluster−ethanol interaction responsible for the frequency shift is local, involving one or a few atoms of the metal cluster, rather than global, involving the total valence electron population. That only a single gold atom is directly involved in the Au_n-C_2H_5OH bond is supported by detailed calculations, discussed below.

4.3. Theoretical Analysis. To begin this discussion of the structure bonding and properties of the gold cluster−ethanol adducts we begin by a brief examination of the isomers of the Au_3 cluster as obtained from electronic structure calculations. Both the BP86 and MP2 level calculations find that the lowest energy isomer of this cluster is that of an isosceles triangle (C_{2v} symmetry) with two Au−Au bonds of about 2.6 Å and a third longer bond of about 2.8−2.9 Å. The open triangle isomer of Au_3 reported in ref 46 is also a stable isomer with respect to the PB86 method in the present work; however, it is found to be about 0.05 eV higher in energy then the ground state. It is noted that this is essentially iso-energetic with the ground state within the accuracy of the current approach. Alternately, one may consider the linear Au_3 molecule with two Au−Au bonds of about 2.6 Å which is not a stable species but rather exhibits two negative vibrational frequencies as obtained with both methods. In this respect MP2 and BP86 are in accord with only the slight exception that the former places the linear species 0.3 eV higher in energy than the ground state as opposed to the 0.1 eV obtained by the latter. The IP as obtained by subtracting the total electronic energy of the neutral and positively charged clusters differ significantly between the approaches with a value of about 7.4 eV for the DFT method and 6.3 eV for MP2. In this respect it appears that the MP2 method underestimates the IP of the pure cluster relative to experiment though one would not expect greater accuracy of this quantity given the approximate nature of the calculation. It is noted, however, that both methods find a less than 0.1 eV dependence of this result upon the structure of the cluster as measured by re-optimizing the geometry of the cation.

Likewise, there is substantial agreement between the two approaches regarding the structure and vibrational frequencies of the free alcohol molecules. Both methods find a C−O bond length of approximately 1.43 Å in both methanol and ethanol. In accordance with experiment the harmonic stretching frequency for methanol is a pure mode (BP86:1016 cm^{-1}, MP2: 1088 cm^{-1}), whereas, for ethanol (anti conformer) this mode is mixed with other modes, C−C stretching as well as H−C−H bending, but has a major contribution to the two frequencies in a similar energy regime (1005 and 1071 cm^{-1} for BP86, 1068, and 1140 cm^{-1} for MP2). In going from the anti to the gauche conformer, the lower frequency shifts upward by 5−20 cm^{-1}, while the higher frequency shifts downward by 15−26 cm^{-1}, depending on the particular theoretical method used. The calculated dipole moment for both alcohols is slightly overestimated by MP2 which gives 1.91 D for methanol (1.70 D experimentally[58]) and 1.79 D for ethanol in the anti conformation (1.44 D experimentally[58]). The BP86 method on the other hand provides dipole moments that are within 0.1 D of the experimental values: 1.66 D for methanol and 1.54 D for ethanol (anti conformer). Thus, both methods predict the correct trends in the behavior of both dipole moments as well as vibrational frequencies between the methanol and ethanol.

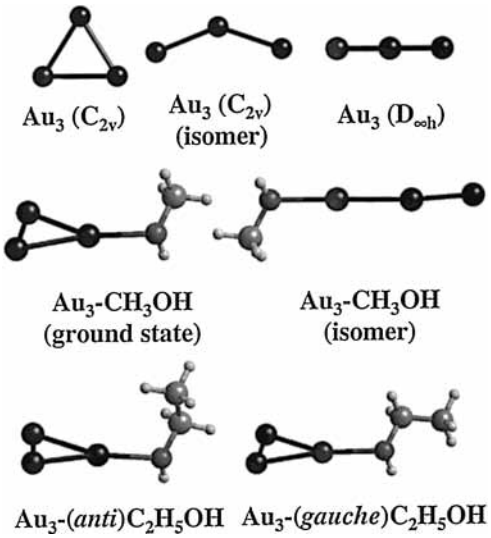

Figure 5. Structure of Au_3 isomers and their adducts formed with methanol and ethanol. Atoms positions are represented by spheres: Au (black), O(dark gray), C(medium gray), and H(small light gray).

Adducts formed by attaching an alcohol to either symmetry-independent Au atom of the C_{2v} ground states result in the same stable adduct where the Au cluster core rearranges into a triangle with three inequivalent edges with Au−Au distances between 2.6 and 2.8 Å (See Figure 5). In these adducts a direct Au−O bond is formed with a distance of 2.28 Å for BP86 and 2.23 A for MP2. This goes hand-in-hand with the slightly larger binding energy of 0.96 eV for MP2 as opposed to the 0.86 eV for BP86. It is noted that both these estimates exceed the values of the binding energies quoted above for gold surfaces. Whether this is a result of the small size of the cluster or a limitation of the theory is as yet an open issue beyond the scope of the current work. It is also possible to obtain a stable isomer of the linear Au_3 cluster by attaching the alcohol to one of the two terminal atoms of the trimer (see Figure 5). This Au_3 portion of the adduct is only slightly bent with an Au−Au−Au bond angle of about 170° and may thus also be thought of as an adduct formed from the open triangle isomer of Au_3.[46] Attaching the alcohol to the central Au atom results in the same isomer obtained from the C_{2v} species. The total energy of this adduct is higher than the ground state (0.1 eV BP86 and 0.2 eV MP2) but exhibits an almost identical binding. Finally, in terms of Au−O bond length and binding energy there is almost no appreciable difference between the adducts formed between methanol and ethanol. Thus, like methanol, ethanol forms a stable adduct with the dipole moment oriented down toward the Au_3 cluster in accord

with the experimental conclusion based upon the lowering of the IP and qualitatively similar to the situation found in charged Au_3^+−methanol adduct.[34]

Upon adsorption onto Au_3 the C−O stretching frequency for the methanol remains a relatively pure vibrational mode and is found to red shift by about 50 cm^{-1} for both theoretical methods employed. The predicted red shift exceeds the 25−30 cm^{-1} of both the theoretical estimate of ref 34 and the experimental work of ref 9. A red shift of the ethanol vibrational bands containing large C−O stretching components is also observed with a range of 4−10 cm^{-1} for the lower frequency band and 40−50 cm^{-1} for the higher (depending on both method and conformation used). Likewise, the IP of the adducts are also lowered by about 0.8 eV by BP86 and 0.6 eV by MP2. There is essentially no difference in the shift for ethanol as opposed to methanol within the accuracy of the calculation and the shift is insensitive to the conformation of ethanol used in the calculation. Thus, the proposed binding model *qualitatively* accounts for the trends in both C−O stretching frequency as well as the observed lowering of the ionization potential. Assuming similar errors in frequency shifts between the two alcohols and that anti−gauche interconversion does not occur at the experimental temperature, then our analysis lends support of the assignment of the adsorbed species as the gauche conformer. Unfortunately, the uncertainties in the calculated vibrational frequencies and their adsorption-induced shifts preclude a definitive identification of the Au_n-adsorbed ethanol as anti or gauche.

The relative insensitivity of the results to the fine details of the adduct structure indicates that, unlike the alcohol adducts of positively charged Au_n^+ clusters,[34] the neutral species will be less sensitive to where the molecule is attached to the cluster. This is also in agreement with the above interpretation of the photodissociation spectra. Although the alcohol-neutral gold cluster interaction is local in nature, it is not as sensitive as that found in the charged species such that the properties of the complex are less influenced by where the molecule is attached to the cluster. A rational for this observation may be found in the charge distribution within the gold cluster. For neutral species only a small local positive charge, of about 0.1e, as measured by Mulliken population analysis, is induced on the Au atom to which the oxygen is bound. This is accompanied by a moderate negative charge buildup on the other Au atoms. In contrast, for Au_3^+−methanol it was found[34] that a large, 0.6e, positive charge was located on the analogous site resulting from the localization of the already existing positive charge of the cluster. Thus, induction of charge by alcohol adsorption on a neutral cluster leads to a less sensitive interaction then the localization of charge induced by alcohol adsorption onto the cationic clusters.

5. Conclusions

The 193 nm photoionization TOF mass spectra together with the photodissociation spectra show that on Au_n, ethanol adsorbs intact, with its dipole moment oriented toward the cluster. In particular, we observe no correlation of the ethanol vibrational band positions with the large electronic and geometric structure variations displayed by the underlying gold clusters, confirming that the interaction responsible for the shift from the gas-phase value is local rather than global. These observations correlate well with a theoretical model in which a simple alcohol molecule is attached to a single Au atom via a direct Au−O bond similar to that found in coordination complexes. Furthermore, this same model correctly reproduces the trends in vibrational spectra and IP charge relative to the free gas-phase cluster and alcohol. The blue shift and broadening of the vibrational bands with increasing ethanol coverage may reflect a strong interaction among the ethanol molecules.

Acknowledgment. The experimental portion of this work is supported by the U.S. Department of Energy, Office of Basic Energy Sciences, Division of Chemical Sciences, under Contract No. W-31-109-ENG-38.

References and Notes

(1) Knickelbein, M. B. *Annu. Rev. Phys. Chem.* **1999**, *50*, 79.
(2) Ervin, K. M. *Int. Rev. Phys. Chem.* **2001**, *20*, 127.
(3) Morse, M. D.; Geusic, M. E.; Heath, J. R.; Smalley, R. E. *J. Chem. Phys.* **1985**, *83*, 2293.
(4) Leuchtner, R. E.; Harms, A. C.; Castleman, A. W., Jr. *J. Chem. Phys.* **1990**, *92*, 6527.
(5) Andersson, M.; Persson, J. L.; Rosén, A. *J. Phys. Chem.* **1996**, *100*, 12222.
(6) Nygren, M. A.; Siegbahn, P. E. M.; Jin, C.; Guo, T.; Smalley, R. E. *J. Chem. Phys.* **1991**, *95*, 6181.
(7) Koretsky, G. M.; Knickelbein, M. B. *Chem. Phys. Lett.* **1997**, *267*, 485.
(8) Irion, M. P.; Selinger, A. *Chem. Phys. Lett.* **1989**, *158*, 145.
(9) Knickelbein, M. B.; Koretsky, G. M. *J. Phys. Chem. A* **1998**, *102*, 580.
(10) Katakuse, I.; Ichihara, T.; Fujita, Y.; Matsuo, T.; Sakurai, T.; Matsuda, H. *Int. J. Mass Spectrom. Ion Processes* **1985**, *67*, 229.
(11) Alameddin, G.; Hunter, J.; Cameron, D.; Kappes, M. M. *Chem. Phys. Lett.* **1992**, *192*, 122.
(12) Knickelbein, M. B. *Chem. Phys. Lett.* **1992**, *192*, 129.
(13) Taylor, K. J.; Pettiette-Hall, C. L.; Cheshnovsky, O.; Smalley, R. E. *J. Chem. Phys.* **1992**, *96*, 3319.
(14) Ho, J.; Ervin, K. M.; Lineberger, W. C. *J. Chem. Phys.* **1990**, *93*, 6987.
(15) Handschuh, H.; Cha, C.-Y.; Möller, H.; Bechthold, P. S.; Ganteför, G.; Eberhardt, W. *Chem. Phys. Lett.* **1994**, *227*, 496.
(16) Clemenger, K. *Phys. Rev. B* **1985**, *32*, 1359.
(17) Brack, M. *Rev. Mod. Phys.* **1993**, *65*, 677.
(18) de Heer, W. A. *Rev. Mod. Phys.* **1993**, *65*, 611.
(19) Martin, T. P.; Bergmann, T.; Göhlich, H.; Lange, T. *J. Phys. Chem.* **1991**, *95*, 6421.
(20) Spasov, V. A.; Lee, T.-H.; Ervin, K. A. *J. Chem. Phys.* **2000**, *112*, 1713.
(21) Wallace, W. T.; Whetten, R. L. *J. Phys. Chem. B* **2000**, *104*, 10964.
(22) Winter, B. J.; Parks, E. K.; Riley, S. J. *J. Chem. Phys.* **1991**, *94*, 8618.
(23) Salisbury, B. E.; Wallace, W. T.; Whetten, R. L. *Chem. Phys.* **2000**, *262*, 131.
(24) Calaminici, P.; Köster, A. M.; Russo, N.; Salahub, D. R. *J. Chem. Phys.* **1996**, *105*, 9546.
(25) Massobrio, C.; Pasquarello, A.; Car, R. *Chem. Phys. Lett.* **1995**, *238*, 215.
(26) Jackson, K. A. *Phys. Rev. B* **1993**, *47*, 9715.
(27) Kaplan, I. G.; Santamaria, R.; Novaro, O. *Int. J. Quantum Chem.* **1993**, *27*, 743.
(28) Bonacic-Koutecky, V.; Cespiva, L.; Fantucci, P.; Koutecky, J. *J. Chem. Phys.* **1993**, *98*, 7981.
(29) Balasubramanian, K. *J. Mol. Struct. (THEOCHEM)* **1989**, *202*, 291.
(30) Wilson, N. T.; Johnston, R. L. *Eur. Phys. J. D* **2000**, *12*, 161.
(31) Dietrich, G.; Dasgupta, K.; Krückeberg, S.; Lützenkirchen, K.; Schweikhard, L.; Walther, C.; Ziegler, J. *Chem. Phys. Lett.* **1996**, *259*, 397.
(32) Rousseau, R.; Dietrich, G.; Krückeberg, S.; Lützenkirchen, K.; Marx, D.; Schweikhard, L.; Walther, C. *Chem. Phys. Lett.* **1998**, *295*, 41.
(33) Dietrich, G.; Krückeberg, S.; Lützenkirchen, K.; Schweikhard, L.; Walther, C. *J. Chem. Phys.* **2000**, *112*, 752.
(34) Rousseau, R.; Marx, D. *J. Chem. Phys.* **2000**, *112*, 761.
(35) Knickelbein, M. B. *J. Chem. Phys.* **1996**, *104*, 3517.
(36) Frisch, M. J.; Trucks, G. W.; Schlegel, H. B.; Scuseria, G. E.; Robb, M. A.; Cheeseman, J. R.; Zakrzewski, V. G.; Montgomery, J. A., Jr.; Stratmann, R. E.; Burant, J. C.; Dapprich, S.; Millam, J. M.; Daniels, A. D.; Kudin, K. N.; Strain, M. C.; Farkas, O.; Tomasi, J.; Barone, V.; Cossi, M.; Cammi, R.; Mennucci, B.; Pomelli, C.; Adamo, C.; Clifford, S.; Ochterski, J.; Petersson, G. A.; Ayala, P. Y.; Cui, Q.; Morokuma, K.; Malick, D. K.; Rabuck, A. D.; Raghavachari, K.; Foresman, J. B.; Cioslowski, J.; Ortiz, J. V.; Stefanov, B. B.; Liu, G.; Liashenko, A.; Piskorz, P.; Komoromi, I.; Gomperts, R.; Martin, R. L.; Fox, D. J.; Keith, T.; Al-Laham, M. A.; Peng, C. Y.; Nanayakkara, A.; Gonzalez, C.; Callacombe, M.; Gill, P. M.; Johnson, B.; Chen, W.; Wong, M. W.; Andres, J. L.; Gonzales, C.; Head-Gordon, M.; Replogle, E. S.; Pople, J. A. *Gaussian 98*; Gaussian Inc.: Pittsburgh, PA, 1998.

(37) Andrae, D.; Haeussermann, U.; Dolg, M.; Stoll, H.; Preuss, H. *Theor. Chim. Acta* **1990**, *77*, 123.
(38) McLean, A. D.; Chandler, G. S. *J. Chem. Phys.* **1980**, *72*, 5639.
(39) Krishnan, R.; Binkley, J. S.; Pople, J. A. *J. Chem. Phys.* **1980**, *72*, 650.
(40) Clark, T.; Chandrasekhar, J.; Spitznagel, G. W.; Shleyer, P. v. R. *J. Comput. Chem.* **1983**, *4*, 294.
(41) Parr, R. G.; Yang, W. *Density-Functional Theory of Atoms and Molecules*; Oxford University Press: Oxford, 1989.
(42) Jones, R. O.; Gunnarson, O. *Rev. Mod. Phys.* **1989**, *61*, 689.
(43) Becke, A. D. *Phys. Rev. A* **1988**, *38*, 3098.
(44) Perdew, J. P. *Phys. Rev. B* **1986**, *33*, 8822.
(45) Head-Gordon, M.; Pople, J. A.; Frisch, M. J. *Chem. Phys. Lett.* **1988**, *153*, 503.
(46) Krüger, D.; Fuchs, H.; Rousseau, R.; Marx, D.; Parrinello, M. *J. Chem. Phys.*, in press.
(47) Collings, B. A.; Athanassenas, K.; Lacombe, D.; Rayner, D. M.; Hackett, P. A. *J. Chem. Phys.* **1994**, *101*, 3506.
(48) Knickelbein, M. B.; Yang, S.; Riley, S. J. *J. Chem. Phys.* **1990**, *93*, 94.
(49) Knickelbein, M. B.; Menezes, W. J. C. *J. Chem. Phys.* **1991**, *94*, 4111.
(50) Outka, D. A.; Madix, R. J. *J. Vac. Sci. Technol. A* **1983**, *3*, 1680.
(51) Perchard, J.-P.; Josien, M.-L. *J. Chim. Phys.* **1968**, *65*, 1834.
(52) Coussan, S.; Bouteiller, Y.; Perchard, J. P.; Zheng, W. Q. *J. Phys. Chem. A* **1998**, *102*, 5789.
(53) Ehbrecht, M.; Huisken, F. *J. Phys. Chem. A* **1997**, *101*, 7768.
(54) Barnes, A. J.; Hallam, H. E. *Trans. Faraday Soc.* **1970**, *66*, 1932.
(55) Flad, J.; Igel-Mann, G.; Preuss, H.; Stoll, H. *Chem. Phys.* **1984**, 90, 257.
(56) Bauschlicher, C. W., Jr.; Langhoff, S. R.; Partridge, H. *J. Chem. Phys.* **1990**, *93*, 8133.
(57) Liao, D.-W.; Balasubramanian, K. *J. Chem. Phys.* **1992**, *97*, 2548.
(58) *Handbook of Chemistry and Physics*, 74 ed.; Lide, D. R., Ed.; CRC: Boca-Raton, 1994.